Current Biology *18*, 1802–1808, November 25, 2008 ©2008 Elsevier Ltd All rights reserved DOI 10.1016/j.cub.2008.10.044

Report

# The GTPase-Activating Protein GRAF1 Regulates the CLIC/GEEC Endocytic Pathway

**Richard Lundmark,[1,3,4,*] Gary J. Doherty,[1,3] Mark T. Howes,[2] Katia Cortese,[2] Yvonne Vallis,[1] Robert G. Parton,[2] and Harvey T. McMahon[1,*]**

[1]Medical Research Council
Laboratory of Molecular Biology
Hills Road
Cambridge, CB2 0QH
UK

[2]Institute for Molecular Bioscience and
Centre for Microscopy and Microanalysis
University of Queensland
Brisbane, Queensland 4072
Australia

## Summary

**Clathrin-independent endocytosis is an umbrella term for a variety of endocytic pathways that internalize numerous cargoes independently of the canonical coat protein Clathrin [1, 2]. Electron-microscopy studies have defined the pleiomorphic *CL*athrin-*I*ndependent *C*arriers (CLICs) and *G*PI-*E*nriched *E*ndocytic *C*ompartments (GEECs) as related major players in such uptake [3, 4]. This CLIC/GEEC pathway relies upon cellular signaling and activation through small G proteins, but mechanistic insight into the biogenesis of its tubular and tubulovesicular carriers is lacking. Here we show that the Rho-GAP-domain-containing protein GRAF1 marks, and is indispensable for, a major Clathrin-independent endocytic pathway. This pathway is characterized by its ability to internalize bacterial exotoxins, GPI-linked proteins, and extracellular fluid. We show that GRAF1 localizes to PtdIns(4,5)P2-enriched, tubular, and punctate lipid structures via N-terminal BAR and PH domains. These membrane carriers are relatively devoid of caveolin1 and flotillin1 but are associated with activity of the small G protein Cdc42. This study provides the first specific noncargo marker for CLIC/GEEC endocytic membranes and demonstrates how GRAF1 can coordinate small G protein signaling and membrane remodeling to facilitate internalization of CLIC/GEEC pathway cargoes.**

## Results and Discussion

The protein *G*TPase *R*egulator *A*ssociated with *F*ocal Adhesion Kinase-1 (GRAF1) is predicted to comprise an N-terminal BAR domain, a PH domain, a RhoGAP domain, a proline-rich domain, and a C-terminal SH3 domain (Figure 1A). GRAF1 exhibits GAP activity for the small G proteins RhoA and Cdc42 and has been shown to interact with the kinases FAK and PKNβ [5, 6, 14]. The presence of a predicted BAR domain in GRAF1 suggests that it might function in membrane sculpting [7]. GRAF1 was found to be expressed in a variety of cell lines (Figure S1A), and by immunocytochemistry we found that GRAF1 was predominantly localized to pleiomorphic tubular and punctate structures in HeLa and NIH 3T3 cells (Figures 1B–1D and Figure S1B). Although GRAF1 can be found primarily on long tubules in some cells, other cells within the same population exhibit a predominantly punctate GRAF1 localization. GRAF1-positive tubules are disrupted at low temperatures, and a 37°C fixation was required for their integrity to be preserved (Figure S1C). Upon monitoring both GRAF1 localization and endocytosis of either the plasma membrane marker DiI or the fluid-phase marker dextran by confocal microscopy, we found that endocytic structures extensively colocalized with GRAF1 (Figures 1B and 1C). Colocalization of GRAF1 was even evident when only very early endocytic structures were examined, indicative of an early endocytic role for GRAF1-positive membranes (Figure 1D). We then examined the turnover of GRAF1-positive membranes with time by overexpressing GFP-tagged full-length GRAF1 in HeLa cells and examining its localization by using four-dimensional spinning-disc confocal microscopy. We found GRAF1-positive tubular structures to be spectacularly dynamic (Figure 1E and Movie S1). By electron microscopy, we found that GRAF1-labeled tubules were around 40 nm in diameter in vivo (Figure 1G). We also found that overexpressed GFP-tagged GRAF1 BAR+PH protein (missing the GAP, proline-rich, and SH3 domains) also labeled tubular membranes that could accumulate DiI (Figure 1F, Movie S2, and data not shown). However, these tubules were much more static than those labeled by overexpressed full-length GRAF1, suggesting that GRAF1 BAR+PH might act in a dominant-negative manner to stabilize early endocytic tubules (see also below).

To examine the specific properties of the predicted lipid-binding region of GRAF1, we performed lipid cosedimentation assays with purified GRAF1 BAR+PH protein (Figure 2A). Using liposomes of varying diameter, we found that GRAF1 BAR+PH bound better to smaller (more highly curved) liposomes, consistent with the presence of a membrane-curvature-sensing BAR domain [7]. Furthermore, we examined the effects of mutating key lysine residues [7] in the BAR domain to glutamates (KK131/132EE) and found that this mutant was now cytoplasmically distributed (Figure S1D). Expression of the BAR domain alone in cells resulted in a predominantly cytoplasmic and sometimes punctate localization (Figure S1E), suggesting that both the BAR and PH domains are necessary for tubular localization of GRAF1. We therefore tested whether, in addition to a curvature-sensing or -generating capability, the GRAF1 BAR+PH unit has phosphoinositide-binding specificity. GRAF1 BAR+PH protein was subjected to lipid cosedimentation assays with 10% phosphatidylserine-containing liposomes with varying phosphoinositide composition (Figure 2B). Greatest binding was observed for PtdIns(4,5)P2-enriched liposomes. PtdIns(4,5)P2 is plasma-membrane enriched [8], consistent with our observations that GRAF1-associated trafficking occurs from this site. GRAF1 BAR+PH protein was also capable of generating tubules in vitro from spherical liposomes as examined by electron microscopy

*Correspondence: richard.lundmark@medchem.umu.se (R.L.), hmm@mrc-lmb.cam.ac.uk (H.T.M.)
[3]These authors contributed equally to this work
[4]Present address: Department of Medical Biochemistry and Biophysics, Umeå University, 901 87 Umeå, Sweden

under negative-staining conditions (Figure 2C). The diameter of these tubules was around 40 nm, consistent with the observed diameter of GRAF1-positive tubules found in cells (Figure 1G). Taken together, these data strongly suggest that the BAR and PH domains of GRAF1 function together to produce and/or stabilize endocytic tubules in vivo.

To identify interacting partners for GRAF1, we immunoprecipitated GRAF1 from rat brain cytosol. Interestingly, GRAF1 was found in a complex with the membrane scission protein Dynamin1 (Figure 2D and S2A). We confirmed binding to both Dynamin1 and Dynamin2 by using GST-tagged GRAF1 SH3 domain as bait in pull-down experiments against purified Dynamin1, brain cytosol, or HeLa cell lysate (Figure 2E; also Figures S2B and S2C). Monomeric GRAF1 SH3 domain was found to bind to a peptide from Dynamin1 proline-rich domain with a $k_d$ of 106 $\mu$M (Figure S2D). Furthermore, treatment of HeLa cells with dynasore resulted in a profound reduction of tubular endocytosis in HeLa cells and a redistribution of GRAF1 to basally located puncta (Figure S2E). These data, taken together with our observation that C-terminally truncated versions of GRAF1 (lacking the SH3 domain) are found on long static tubules, suggests that the complex between Dynamin and GRAF1 might function to regulate the scission and stability of these ordinarily pleiomorphic tubulovesicular structures.

Clathrin polymers are rarely found on tubular membranes by electron microscopical techniques. Indeed, GRAF1-positive tubules, and other GRAF1-positive structures, were devoid of Clathrin and did not colocalize with internalized or internalizing transferrin or the transferrin receptor, which is widely used as a marker for Clathrin-mediated endocytic events (Figures S3A–S3C). Alongside the canonical Clathrin-mediated endocytic routes, other prevalent endocytic pathways coexist [1, 2]. For example, the internalization of MHC class I proteins, many GPI-linked receptors, and bacterial exotoxins rely on trafficking compartments with heretofore undefined coat components. The data presented above strongly suggest that GRAF1 might function as a coat within a prevalent Clathrin-independent endocytic pathway. To characterize further the nature of GRAF1-positive tubules, we incubated GRAF1-overexpressing HeLa cells with cholera toxin B subunit (CTxB), a marker that is used for the study of Clathrin-independent endocytic pathways but that also enters via Clathrin-mediated routes [9]. We found that internalized CTxB colocalized with Myc-GRAF1-positive tubules in HeLa cells (Figure 2F) as well as with endogenous GRAF1-positive structures after 5 min incubation at 37°C (Figure 2G). In addition, we found that GRAF1 BAR+PH overexpression (which leads to static tubules; Figure 1F) halved the number of cells internalizing CTxB without effecting transferrin uptake (Figures S4A–S4C). We then followed CTxB and transferrin internalization in real time in NIH 3T3 cells (almost all of which are capable of binding and internalizing CTxB; cf. HeLa cells, which often lack its glycolipid receptor, GM1). NIH 3T3 cells were transfected with constructs encoding either GFP-tagged GRAF1 or GRAF1 BAR+PH and incubated with CTxB and transferrin on ice before stimulation of endocytosis by incubation of cells with prewarmed (37°C) media. Imaging commenced immediately (Figure S4D and Movie S3). Newly forming dynamic GRAF1-positive tubules were shown to contain CTxB at extremely early stages of its internalization and were unassociated with internalizing/internalized transferrin. Furthermore, the more static, elongated GRAF1 BAR+PH-positive tubules maintained the presence of CTxB, again independently of transferrin, suggesting that here the toxin is trapped in structures that cannot undergo fission from the plasma membrane and progress further (data not shown).

Although GRAF1-positive carriers resemble the previously characterized Arf6-dependent structures that are responsible for uptake of MHC Class I proteins [10], we found no evidence for overlap between these pathways. Neither GRAF1- nor GRAF1 BAR+PH-positive tubules were found to contain endocytosed or recycled MHC class I proteins at 5, 15, or 45 min after stimulation of their internalization when specific antibodies were used, and the amount of total MHC class I protein endocytosis was not altered upon overexpression of the dominant-negative GRAF1 BAR+PH construct (Figures S6A and S6B and data not shown). In addition, the tubular localization of GRAF1 was independent of overexpression of wild-type Arf6 or dominant-active Arf6 (Arf6Q67L; data not shown). In contrast, Arf6 Q67L overexpression was found to completely block the internalization of MHC class I molecules ([11] and data not shown).

Electron-microscopy studies, focusing on the uptake of CTxB and GPI-linked receptors, have suggested that a large portion of these proteins are internalized by *C*lathrin-*i*ndependent *c*arriers (CLICs) seemingly into *G*PI-AP-enriched *e*arly *e*ndosomal *c*ompartments (GEECs), together with fluid-phase markers such as dextran [4]. Our data have shown that GRAF1-positive structures morphologically and functionally resemble the endocytic structures of this CLIC/GEEC endocytic pathway [4]. We therefore examined whether GRAF1 could regulate the internalization of a model GPI-linked protein known to undergo endocytosis into the CLIC/GEEC pathway. Consistent with this, we found by using immuno-electron microscopy that GRAF1 labeled GFP-GPI-positive tubules (Figure 3A). We then examined the internalization of GFP-GPI in mouse embryonic fibroblasts by binding anti-GFP antibodies and transferrin (as a control) to cells on ice and subsequently moving these cells to 37°C for variable chase periods. We did this in both wild-type (data not shown) and caveolin1-knockout mouse embryonic fibroblasts (to exclude caveolae-associated uptake) that we transfected with either a Myc-tagged GRAF1 or a Myc-tagged GRAF1 BAR+PH construct and examined after cytosol washout (Figure 3B; note that washout treatment damages GRAF1-positive membranes but is necessary for the objective quantitative analysis of colocalization of GRAF1 with internalized GFP-GPI because cytoplasmic GRAF1 would otherwise result in overestimation of colocalization). GRAF1 was found to significantly colocalize with internalized GFP-GPI (79% colocalization) but not transferrin after a 2 min chase (Figures 3B and 3C and data not shown). A reduced level of colocalization was seen after a 10 min chase (47%), and even lower colocalization levels were observed after a 40 min chase (when the protein is recycling back to the plasma membrane; 23%). These data are consistent with our previous observations, strongly suggesting a role for GRAF1 function in sculpting the highly curved membranes of the CLIC/GEEC endocytic pathway. In contrast, GRAF1 BAR+PH consistently colocalized with GFP-GPI after 2 min (60%), 10 min (68%), and 40 min (75%) chase periods, further supporting a role for this protein as a dominant-negative protein that traps early CLIC/GEEC carriers. To characterize this dominant-negative effect in greater detail, we examined the effect of GRAF1 BAR+PH protein on GFP-GPI internalization (Figures 3B and 3C). Compared with GFP-GPI internalization in the presence of GRAF1, the total amount of GFP-GPI internalization was profoundly reduced in the presence of GRAF1 BAR+PH (to around 10% of control levels),

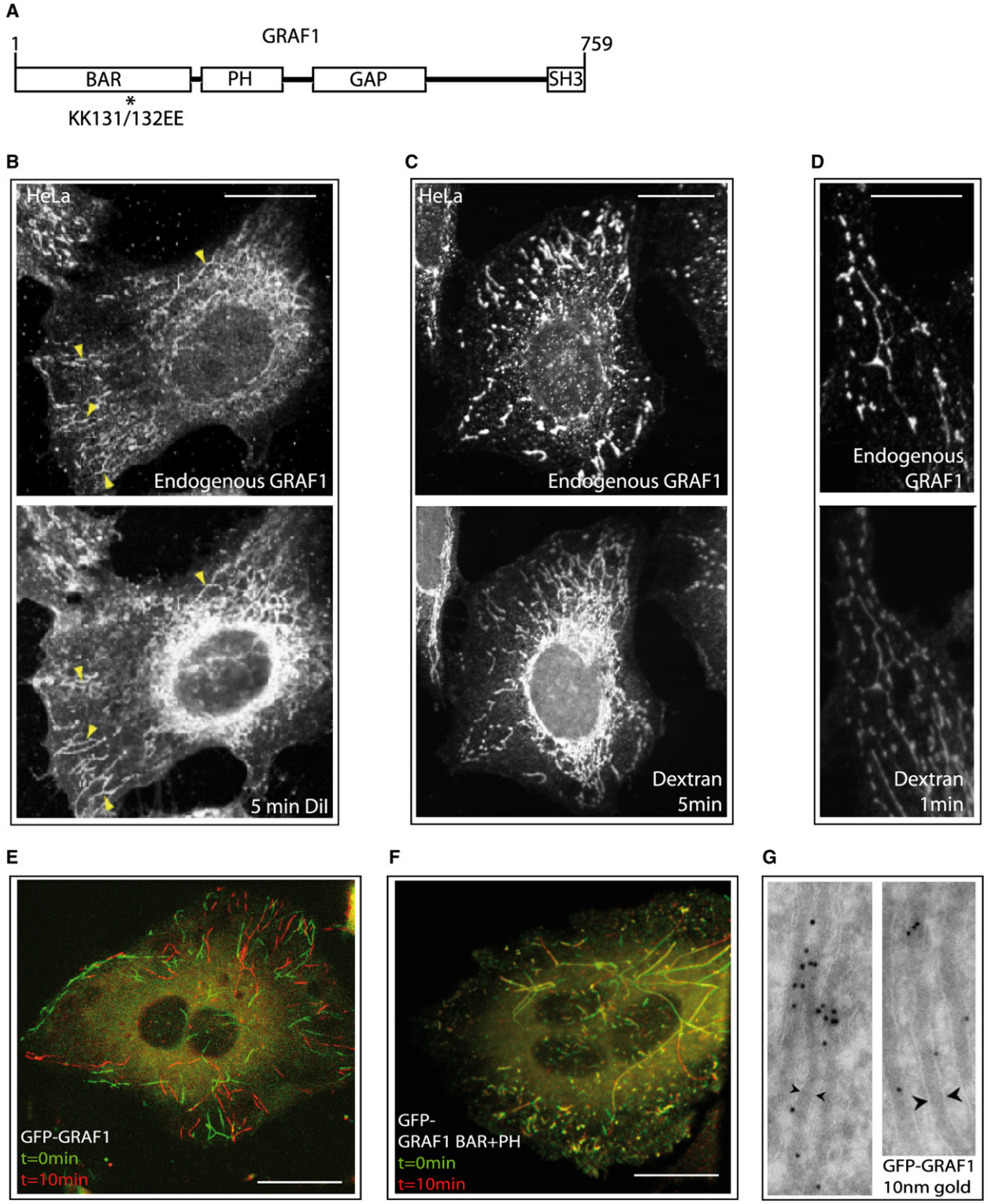


Figure 1. GRAF1 Tubules Are Highly Dynamic and Mark a Prevalent Endocytic Pathway

(A) Domain architecture of GRAF1 and the site of introduced BAR domain mutations (*).

(B–D) Micrographs showing that GRAF1-positive tubules are derived from the plasma membrane as shown by colabeling with the membrane dye DiI after 5 min (B) or internalized dextran after either 5 min (C) or 1 min (D) of incubation.

(E) Overlaid maximum projections of spinning-disc confocal micrographs of HeLa cells expressing GFP-tagged GRAF1 demonstrate that GRAF1-positive tubules are completely turned over in 10 min. Z sections were performed continuously for 10 min in 0.5 μm steps. The initial maximum projection (in green) was then merged with the final maximum projection (in red). See also Movie S1.

(F) Overlaid maximum projections as in (a), but for a cell overexpressing GFP-tagged GRAF1 BAR+PH. See also Movie S2.

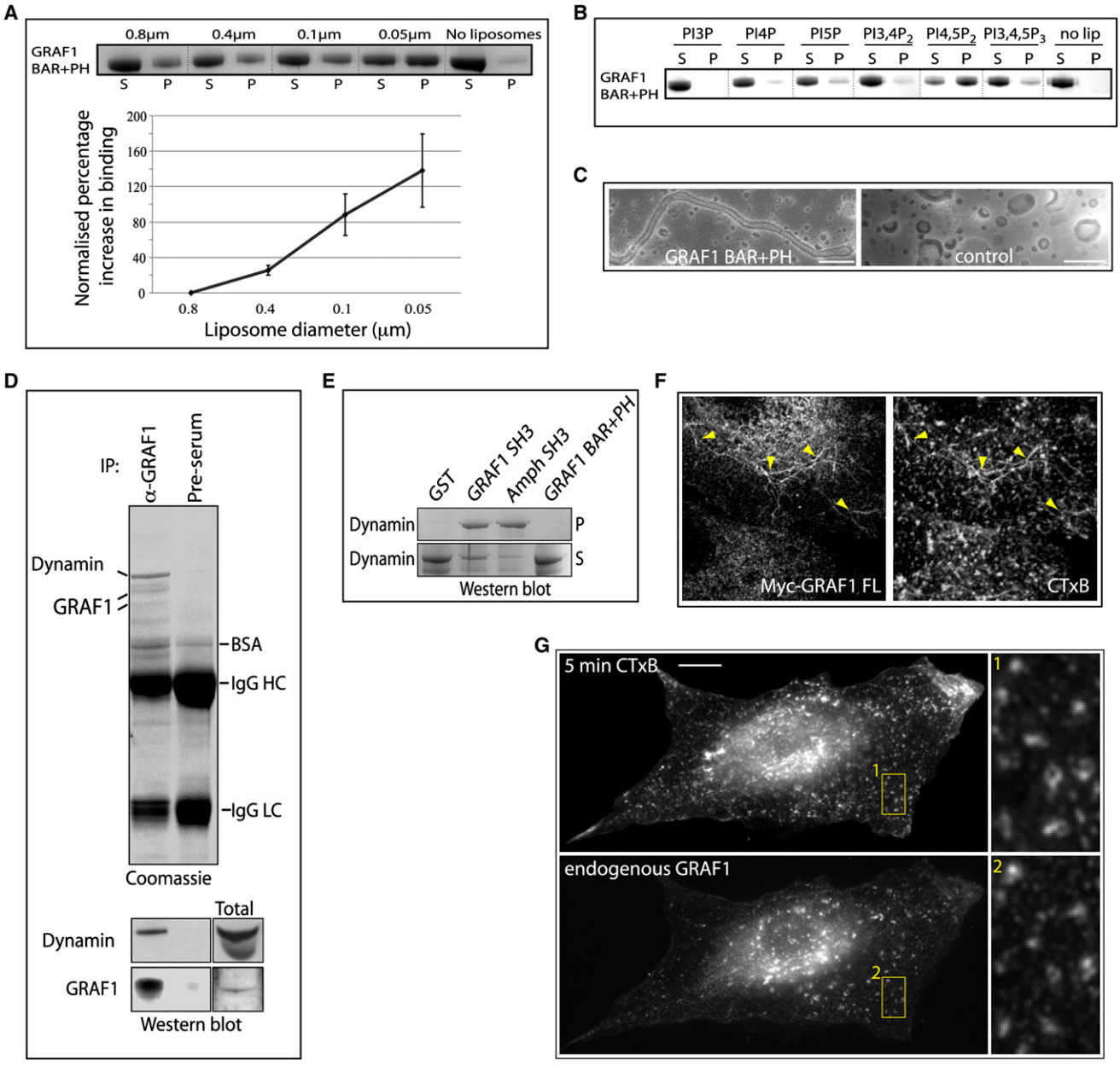


Figure 2. The BAR and PH Domains Localize GRAF1 to Highly Curved, PtdIns(4,5)P2-Enriched Membranes, and the SH3 Domain Binds Dynamin

(A) Coomassie-stained gel of liposome cosedimentation assay showing the preference of GST-tagged GRAF1 BAR+PH protein for binding to smaller-sized liposomes derived from total brain lipids (the average diameters of liposomes are shown). Pellet (P) and supernatant (S) fractions were separated by ultracentrifugation. The graph shows quantifications of total band intensities for each condition normalized to binding of the non-curvature-sensitive protein Dab2 (as a way of controlling for total lipid in each experiment). The error bars show 95% confidence intervals (calculated by t tests) for each condition.

(B) Liposome cosedimentation assay as performed in (A) but with 0.8-μm-diameter liposomes enriched with varying phosphoinositides.

(C) Electron micrographs of negatively stained liposomes incubated in the presence or absence of GST-tagged GRAF1 BAR+PH protein. Note the protein-dependent presence of tubular structures. The scale bar represents 200 nm.

(D) Immunoprecipitation of GRAF1 from rat brain cytosol (via Ab2) reveals a GRAF1-Dynamin1 complex as identified by mass spectrometry and confirmed by immunoblot.

(E) Coomassie-stained gels of pull-down experiments with purified Dynamin and either bead-bound GST-tagged GRAF1/Amphiphysin SH3 domain or GRAF1 BAR+PH protein. P = pellet fraction, S = supernatant fraction.

(F and G) Epifluorescence micrographs of HeLa cell overexpressing Myc-tagged GRAF1 and incubated with CTxB for 5 min before fixation and staining.

(G) Epifluorescence micrographs of a HeLa cell incubated with CTxB for 5 min before fixation and staining for endogenous GRAF1. Scale bars represent 10 μm.

(G) Electron micrographs prepared as described and immunolabeled for GRAF1 (10 nm gold particles). Note the GRAF1-positive tubular structures. Distance between arrowhead tips = 40 nm.

Scale bars represent 10 μm.

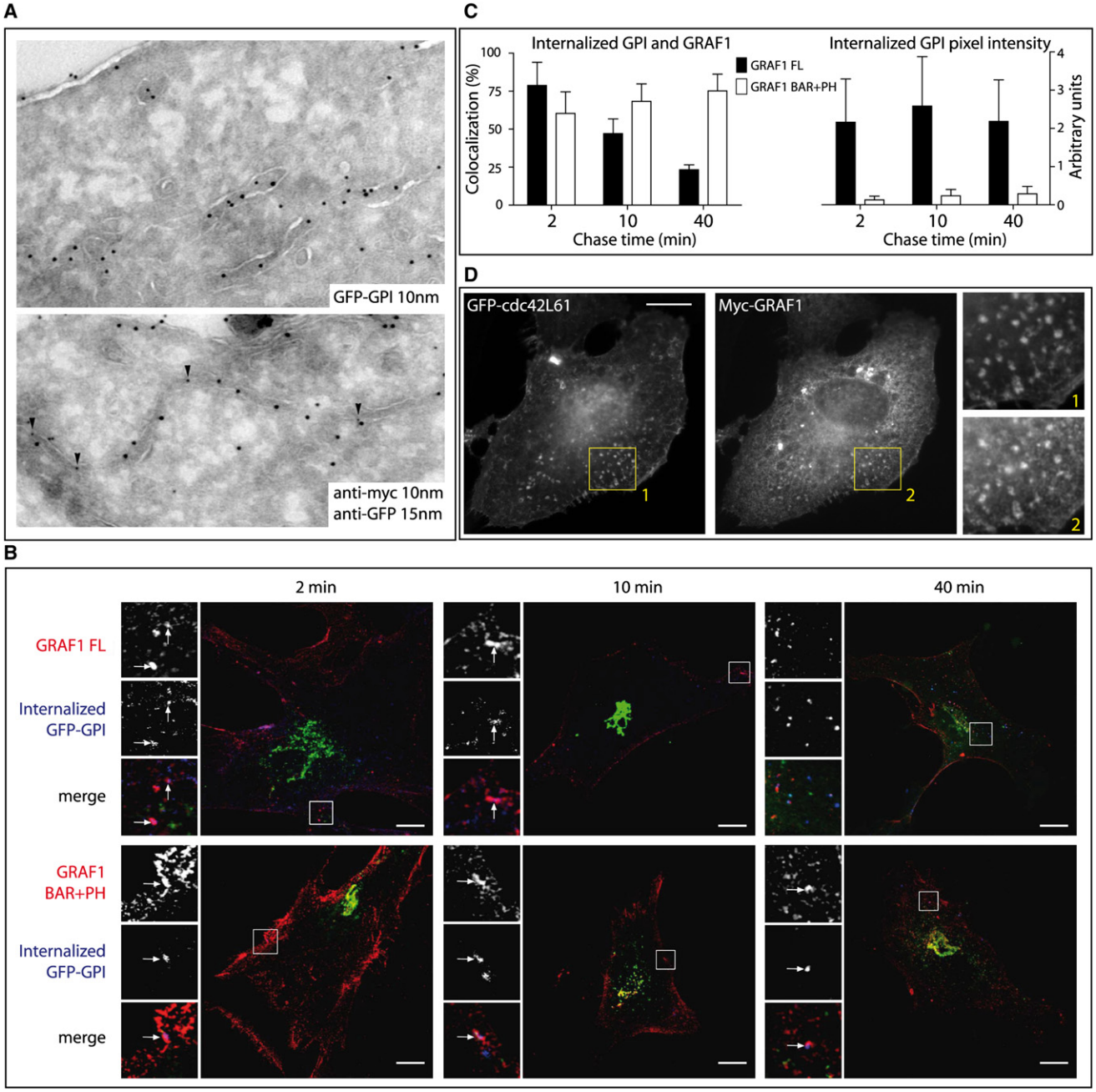


Figure 3. GRAF1 Regulates the CLIC Endocytic Pathway

(A) Representative electron micrographs of 65 nm ultrathin cryosections of HeLa cells transiently transfected with GFP-GPI alone or with both GFP-GPI and Myc-tagged GRAF1 FL. Cells were fixed in 2% PFA with 0.2% glutaraldehyde and labeled with anti-GFP and anti-Myc antibodies. Protein A 10 nm gold was used for revealing the GFP in the single labeling (upper image). As shown, GFP-GPI was found in uncoated vesicles and tubules within the cell. Double labeling of GRAF1 (Protein A gold 10 nm) and GFP-GPI (Protein A gold 15 nm) is shown in the bottom image, where colocalization of GRAF1 and GFP-GPI is seen in an intracellular tubule. Arrowheads point to 10 nm gold particles. Due to limitations of the Tokuyasu method, it is not possible to discriminate cell surface-connected tubules from intracellular tubules.

(B) Caveolin1 knockout MEFs were cotransfected with GFP-GPI (green) and either Myc-tagged GRAF1 (upper row; red) or GRAF1 BAR+PH (lower row; red). GFP antibodies (blue) were bound to cells for 30 min on ice prior to induction of internalization at 37°C and 5% $CO_2$ for the indicated times. Surface labeling was removed, and cytosol extraction followed (see Supplemental Experimental Procedures). Panels on the left side of each image show GRAF1 proteins (top), internalized anti-GFP (middle), and a merged, triple-labeled image (bottom). Arrows indicate points of colocalization.

(C) Micrographs of Caveolin1 knockout MEFs co-overexpressing GRAF1 and GFP-GPI, after anti-GFP internalization, acid stripping, and cytosol extraction, were processed with Volocity 3.7.0 so that the percentage colocalization could be calculated. The histogram shows the number of anti-GFP pixels that colocalize with GRAF1 relative to all anti-GFP pixels. Five to seven images across three independent experiments were taken after 2, 10, and 40 min of internalization. Error bars indicate the standard errors of the mean. Images were also processed in Adobe Photoshop CS2 so that the number of anti-GFP pixels relative to total pixels within the image could be calculated. The histogram represents standardized values of anti-GFP pixels. Error bars indicate the standard errors of the mean.

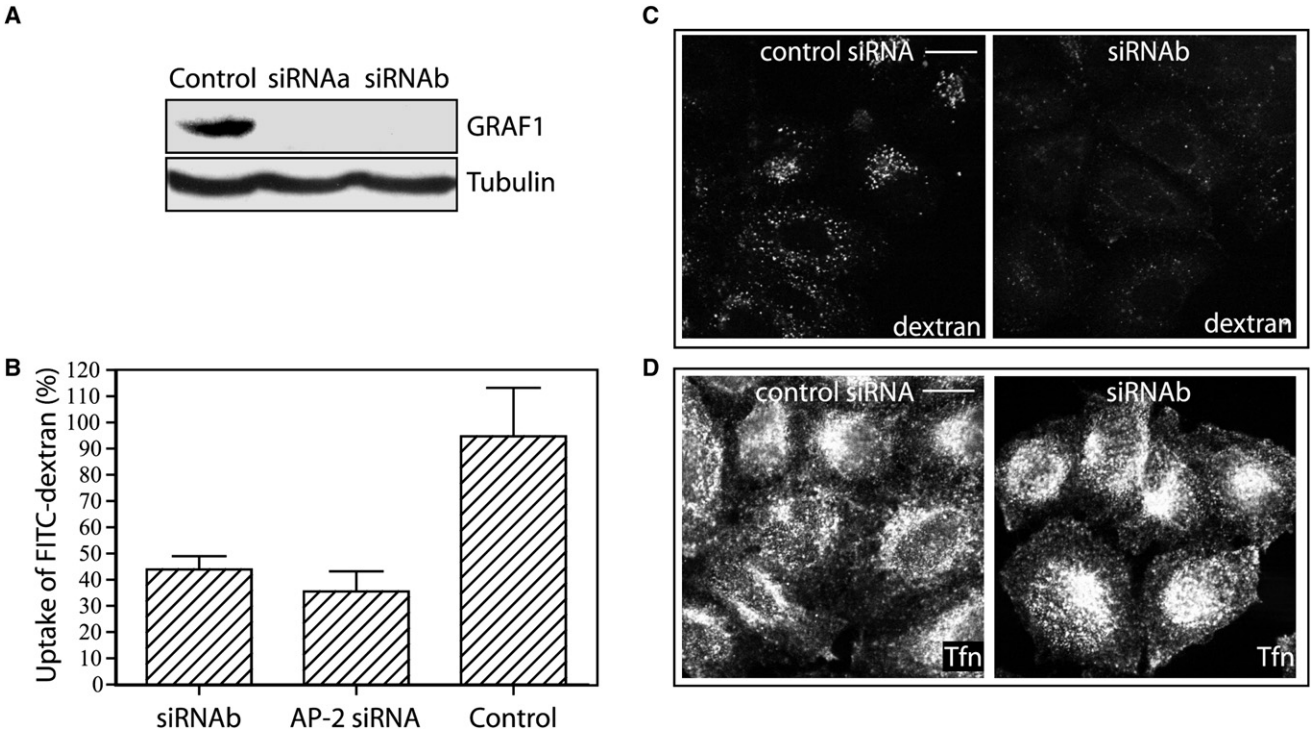


Figure 4. GRAF1 Is Indispensable for Clathrin-Independent Fluid-Phase Uptake in Fibroblasts

(A) Immunoblots on HeLa cell lysates transfected with a control siRNA or either of two siRNAs directed against GRAF1 mRNA (siRNAs a and b). Detection of GRAF1 and tubulin (loading control) was performed with specific antibodies on lysates obtained 48 hr after transfection.

(B) GRAF1-depleted cells show a major reduction in fluid-phase endocytosis as shown by the decrease in the uptake of FITC-labeled dextran (control siRNA (n = 5), siRNAa (n = 8), or AP2 siRNA (n = 3)). The error bars show the standard deviation of the mean.

(C and D) HeLa cells depleted of GRAF1 were incubated with dextran (C) or transferrin (D) for 15 min before fixation and staining.

Scale bars represent 10 μm.

suggesting further that this protein traps cargoes in rather static early endocytic carriers that are incapable of undergoing fission from the plasma membrane. Importantly, the steady-state surface levels of GFP-GPI were indistinguishable between cells expressing GRAF1 and those expressing GRAF1 BAR+PH (Figure S6C).

CTxB has been shown to be endocytosed via caveolin and flotillin-positive structures [12]. Although we did not find caveolin1 or flotillin1 in GRAF1-positive structures at steady state by fluorescence microscopy (Figures S5A and S5B), stabilization of early GRAF1-positive carriers by GRAF1 BAR+PH overexpression caused flotillin1, and to a lesser extent caveolin1, to be found in such regions with CTxB (Figures S5C and S5D), suggesting that these membrane regions can communicate with the CLIC/GEEC pathway.

Uptake through the CLIC/GEEC endocytic pathway has previously been shown to be Cdc42 dependent [3]. Consistent with this, we observed that overexpressed dominant-active Cdc42 protein colocalizes with GRAF1 in basally located puncta (Figure 3D). The absence of Cdc42 in long tubular structures might suggest that the role of Cdc42 in this pathway is restricted spatially and temporarily to the earlier endocytic stages or that progression is blocked through the dominant-active construct, which would be expected to have pleiotropic effects.

To determine whether GRAF1 was necessary for endocytosis, we depleted GRAF1 levels by using siRNA. This treatment was capable of reducing the amount of GRAF1 to background levels as assessed by immunocytochemistry and immunoblotting of HeLa cells and their lysates, respectively (Figure 4A; also Figure S6D). GRAF1-depleted cells were assessed for their ability to endocytose dextran (allowing assessment of total endocytic capacity), both by epifluorescence microscopy and by a quantitative fluorimetric assay (Figures 4B and 4C). GRAF1 depletion resulted in a 50%–60% reduction of total dextran endocytosis, similar to that observed upon depletion of AP2, the major Clathrin adaptor at the plasma membrane (Figure 4B), suggesting that GRAF1-mediated endocytosis and Clathrin-mediated endocytosis account for roughly equal amounts of volume internalization in these cells. GRAF1-depleted cells had no observable defects in their ability to endocytose transferrin (Figure 4D), demonstrating that GRAF1 is not necessary for Clathrin-mediated endocytosis.

In this study we have shown that GRAF1 is found on tubular and vesicular membranes in vivo, and that these membranes define a prevalent Clathrin-independent endocytic pathway. This endocytic pathway is capable of internalizing Cholera toxin, GPI-linked proteins, and large amounts of extracellular fluid, and it corresponds (at least in part) to the CLIC/GEEC endocytic pathway. Activity of Arf1, in addition to that of its GEF

(D) Confocal micrographs of HeLa cells co-overexpressing GFP-tagged Cdc42 L61 (dominant-active) and Myc-tagged GRAF1 showing colocalization in discrete puncta and short tubules.

Scale bars represent 10 μm.

ARHGAP10, is necessary for uptake via the CLIC/GEEC pathway, and Arf1 activity modulation also interferes with Cdc42 dynamics, suggesting interplay between these proteins [13]. Indeed, GRAF1 is capable of downregulating the activity of Cdc42 [14], which is known to be necessary for the CLIC/GEEC pathway [3] and which colocalizes with GRAF1 in vivo. The protein machinery responsible for the biogenesis and processing of CLIC/GEEC endocytic membranes is largely unknown. Although Dynamin certainly plays a role in CLIC/GEEC membrane processing (it is necessary for delivery of CTxB to the Golgi apparatus [4]), its precise role in the CLIC/GEEC pathway is uncertain. Recent microinjection experiments with antibodies directed against specific isoforms of Dynamin, or with siRNAs directed against these, showed that Dynamin is involved in constitutive fluid-phase uptake and suggested that it might play an important role in high-volume Clathrin-independent endocytic events [15]. We build on this work by showing that there exists a tight biochemical interaction between GRAF1 and Dynamin. Although we implicate Dynamin in this pathway, precisely determining whether it functions here in an analogous manner to Dynamin at Clathrin-coated pits or works via a noncanonical mechanism will require further work.

Our experiments lead us to suggest that GRAF1 coordinates the highest volume Clathrin-independent endocytic pathway in HeLa cells. Although several Clathrin-independent endocytic pathways appear to coexist (such pathways include caveolin1- and flotillin1-positive pathways, an Arf6-associated tubular uptake pathway, and the CLIC/GEEC pathway), the precise contributions that each of these pathways makes to constitutive endocytosis, and the interrelationships between these pathways, are uncertain. Although we have found that GRAF1-positive membranes contain little flotillin1 or caveolin1 at steady state, we have also shown that these membranes probably transiently communicate. We further show that GRAF1-positive membranes are not associated with internalizing or recycled MHC class I proteins. Taken together, our data link biochemical and cell biological observations to identify the first important modulator of membrane curvature in a highly prevalent Clathrin-independent endocytic pathway. We believe that, in the context of our findings, study of Clathrin-independent endocytic pathways will reveal new layers of complexity underlying lipid and protein cargo selection, appropriate intracellular trafficking of endocytic membranes, and the mechanisms of endocytic intermediate formation by membrane deformation and membrane-curvature stabilization.

### Supplemental Data

Supplemental Data include Supplemental Experimental Procedures, six figures, and three movies and are available with this article online at http://www.current-biology.com/supplemental/S0960-9822(08)01413-9.

### Acknowledgments

Many thanks to Sew Peak-Chew and Farida Begum for assistance with mass spectrometry analysis, Marijn Ford for providing purified Dynamin, and Sven Carlsson and all members of the McMahon lab for help and support. We also thank the Kempe and Magn Bergvall foundations and Medical faculty Umeå University for grants. Thanks to M. Fällman, B Nichols, J.W.G. Andersson and S. Mayor for providing reagents. R.L was supported by a postdoctoral fellowship from the Swedish Research Council. G.D was supported by a Trinity College Cambridge Internal Graduate Studentship and Research Scholarship. The main work was founded by Medical Research Council UK.

Received: April 7, 2008
Revised: October 4, 2008
Accepted: October 8, 2008
Published online: November 24, 2008

### References

1. Mayor, S., and Pagano, R.E. (2007). Pathways of clathrin-independent endocytosis. Nat. Rev. Mol. Cell Biol. *8*, 603–612.
2. Johannes, L., and Lamaze, C. (2002). Clathrin-dependent or not: is it still the question? Traffic *3*, 443–451.
3. Sabharanjak, S., Sharma, P., Parton, R.G., and Mayor, S. (2002). GPI-anchored proteins are delivered to recycling endosomes via a distinct cdc42-regulated, clathrin-independent pinocytic pathway. Dev. Cell *2*, 411–423.
4. Kirkham, M., Fujita, A., Chadda, R., Nixon, S.J., Kurzchalia, T.V., Sharma, D.K., Pagano, R.E., Hancock, J.F., Mayor, S., and Parton, R.G. (2005). Ultrastructural identification of uncoated caveolin-independent early endocytic vehicles. J. Cell Biol. *168*, 465–476.
5. Hildebrand, J.D., Taylor, J.M., and Parsons, J.T. (1996). An SH3 domain-containing GTPase-activating protein for Rho and Cdc42 associates with focal adhesion kinase. Mol. Cell. Biol. *16*, 3169–3178.
6. Shibata, H., Oishi, K., Yamagiwa, A., Matsumoto, M., Mukai, H., and Ono, Y. (2001). PKNbeta interacts with the SH3 domains of Graf and a novel Graf related protein, Graf2, which are GTPase activating proteins for Rho family. J. Biochem. (Tokyo) *130*, 23–31.
7. Peter, B.J., Kent, H.M., Mills, I.G., Vallis, Y., Butler, P.J., Evans, P.R., and McMahon, H.T. (2004). BAR domains as sensors of membrane curvature: the amphiphysin BAR structure. Science *303*, 495–499.
8. Di Paolo, G., and De Camilli, P. (2006). Phosphoinositides in cell regulation and membrane dynamics. Nature *443*, 651–657.
9. Torgersen, M.L., Skretting, G., van Deurs, B., and Sandvig, K. (2001). Internalization of cholera toxin by different endocytic mechanisms. J. Cell Sci. *114*, 3737–3747.
10. Naslavsky, N., Weigert, R., and Donaldson, J.G. (2004). Characterization of a nonclathrin endocytic pathway: membrane cargo and lipid requirements. Mol. Biol. Cell *15*, 3542–3552.
11. Caplan, S., Naslavsky, N., Hartnell, L.M., Lodge, R., Polishchuk, R.S., Donaldson, J.G., and Bonifacino, J.S. (2002). A tubular EHD1-containing compartment involved in the recycling of major histocompatibility complex class I molecules to the plasma membrane. EMBO J. *21*, 2557–2567.
12. Glebov, O.O., Bright, N.A., and Nichols, B.J. (2006). Flotillin-1 defines a clathrin-independent endocytic pathway in mammalian cells. Nat. Cell Biol. *8*, 46–54.
13. Kumari, S., and Mayor, S. (2008). ARF1 is directly involved in dynamin-independent endocytosis. Nat. Cell Biol. *10*, 30–41.
14. Taylor, J.M., Macklem, M.M., and Parsons, J.T. (1999). Cytoskeletal changes induced by GRAF, the GTPase regulator associated with focal adhesion kinase, are mediated by Rho. J. Cell Sci. *112*, 231–242.
15. Cao, H., Chen, J., Awoniyi, M., Henley, J.R., and McNiven, M.A. (2007). Dynamin 2 mediates fluid-phase micropinocytosis in epithelial cells. J. Cell Sci. *120*, 4167–4177.

# Supplemental Data

# The GTPase-Activating Protein GRAF1

# Regulates the CLIC/GEEC Endocytic Pathway

Richard Lundmark, Gary J. Doherty, Mark T. Howes, Katia Cortese, Yvonne Vallis, Robert G. Parton, and Harvey T. McMahon

## Supplemental Experimental Procedures

### cDNA construct preparation

cDNA constructs encoding human GRAF1 (amino acids 1-759), GRAF1-BAR+PH (amino acids 1-383), GRAF1 PH+GAP (amino acids 267-576), and GRAF1-SH3 (694-759) were amplified from IMAGE clone 30343863 using PCR and cloned into the pGEX- 4T-2 vector for bacterial expression (Amersham Biosciences). GRAF2 SH3 domain was amplified similarly from IMAGE clone 6188298 and cloned into the pGEX-4T-2 vector. Fragments were also cloned into the pCMVmyc vector with added Not1 site (a kind gift from JGW Anderson) or EGFP-C3 (Clontech) for mammalian expression. Amino acid substitutions K131E, K132E and R412D were created using PCR directed mutagenesis (Stratagene). The GFP-tagged Cdc42 L61 consrtruct was a kind gift from M. Fällman. pEGFP-GPI was a generous gift from S. Mayor. caveolin1-GFP and flotillin1-GFP were kind gifts from Ben Nichols.

### Protein expression, protein purification and antibodies

Recombinant proteins were expressed in a BL21 (DE3) pLysS *E-coli* strain as Glutathione S-transferase (GST)- fusion proteins and purified using glutathione-Sepharose 4B beads (Amersham Biosciences) and gel filtration on a sephacryl S-200 column (Amersham) as previously described [1]. Polyclonal antisera against GRAF1 were generated by immunising Rabbits (Ra83/Ab1 directed against the SH3 domain; Ra84/Ab2 directed against the PH+GAP domains; and RaZ1/Ab3 directed against the full length protein; all of these were used for Western blotting analyses, and Ab1/3 also used for immunofluorescence analyses) and a chicken (CH-9798/Ab4, directed against the full length protein, used for immunofluorescence analyses) with recombinantly expressed human GRAF1 proteins. Purchased antibodies were: mouse anti-myc clone 9E10, mouse anti-tubulin (Sigma-Aldrich), Rabbit anti-myc (Cell Signalling Technology), mouse anti-Dynamin, (BD Transduction Laboratories), Rabbit anti-synaptojanin Ra59 [1], (Affinity Bioreagents). All secondary antibodies and streptavidins were conjugated to Alexa Fluor 488, 546 or 647 (Invitrogen).

### Expression, immunoprecipitation and pull down experiments

For analysis of endogenous protein expression, cell lines were grown according to instructions from American Tissue Culture Collection, harvested and lysed in 1% NP-40 in PBS supplemented with protease inhibitors. After a 20,000g centrifugation the supernatant was analysed by SDS-PAGE and immunoblotting. For immunoprecipitation experiments, rat brain cytosol was generated by homogenization of rat brains in buffer (25mM HEPES, 150mM NaCl, 1mM DTT, 0.1% Triton X-100 and protease inhibitors), before centrifugation at 50,000rpm for 30 minutes at 4°C. The supernatant was removed and added to protein A Sephorose 4B beads (Amersham Biosciensis) to which antibodies had been previously bound and incubated at 4°C for 3 hours. Beads were washed three times in buffer (25mM HEPES, 150mM NaCl) supplemented

with 1% NP-40, and once in buffer without NP-40 before analysis by SDS-PAGE combined with immunoblotting or Coomassie staining. Pull-down experiments against rat brain cytosol using purified proteins and identification by mass-spectrometry were performed as previously described [1].

**Protein and lipid interaction assays**

Liposomes from total brain lipids (FOLCH fraction I) (Sigma Aldrich) or synthetic lipids (Avanti Polar Lipids), and liposomes of a specified diameter or phosphoinositide enrichment were generated as previously described [2]. Liposome binding assays for lipid specificity and curvature sensitivity was performed as previously described [2]. Briefly, proteins were incubated together with liposomes followed by centrifugation and analysis of the pellet and supernatant by SDS-PAGE and Coomassie staining. *In vitro* liposome tubulation assays were performed and analysed as previously described [2].

**Isothermal titration calorimetry**

The binding of synthetic peptides from Dynamin1 to purified GRAF1 SH3 domain was measured by isothermal titration calorimetry (ITC) using a VP-ITC (MicroCal Inc., USA). All experiments were performed in 100mM HEPES/NaOH pH 7.4, 50mM NaCl and 2mM DTT at 10°C. Protein concentrations were determined by absorbance at 280nm. 1.36ml of 51μM GRAF1 SH3 domain was loaded into the cell. The peptides (at 1mM which were custom-designed and manufactured at the Institute of Biomolecular Sciences, University of Southampton, UK) were injected from a syringe in 5μl steps every 3.5 minutes. The heat of the dilution of the ligand was subtracted from the data prior to fitting. Titration curves were fitted to the data using the ORIGIN program (MicroCal Inc.) which yielded the stoichiometry (~1), the binary association constant $K_a$ ($=K_d^{-1}$) and the enthalpy of binding. The entropy of binding ($\Delta S°$) was calculated from the relationship $\Delta G° = - RT \bullet \ln(K_a)$ and the Gibbs-Helmholtz equation.

**Cell culture and transfections**

HeLa cells were grown in RPMI 1640 or MEM media (GIBCO) supplemented with LGlutamine, 10% foetal bovine serum, non-essential amino acids (for MEM), and transfected using Genejuice (Novagen) for transient protein expression. For primary cultures, rat hippocampal neurons/astrocytes were prepared by trypsin digestion and mechanical trituration from E18 or P1 Sprague-Dawley rats and plated onto poly L-lysine coated coverslips. Cells were cultured in B27-supplemented Neurobasal media. For GRAF1 depletion, HeLa cells were transfected with Stealth siRNAs specific against human GRAF1 using Lipofectamine 2000 (Invitrogen) according to manufacturers instructions. The Invitrogen siRNA duplex sequences used were siRNAa (UUA UCU CCC AUU CAG CAC AGA UAU C/ GAU AUC UGU GCU GAA UGG GAG AUA A), and siRNAb (UUU GAA ACU GGU ACA UCA UGA GUG G/CCA CUC AUG AUG UAC CAG UUU CAA A). Cells were cultured for an additional 48 hours for efficient silencing of the GRAF1 expression. Stealth Block-it siRNA (Invitrogen) was used as a control. AP2 siRNA was used as previously described [3]. Caveolin-1 knock-out mouse embryonic fibroblasts (KO MEFs) were generated and grown as previously described [4]. NIH 3T3 cells were cultured as per ECACC guidelines.

**Trafficking assays**

For immunofluorescence trafficking assays, biotinylated holo-transferrin, (Sigma Aldrich), Alexa Fluor 647-conjugated transferrin (Invitrogen), Alexa Fluor 546/555- conjugated CTxB (Invitrogen), DiI (Invitrogen), FITC-dextran (10kDa MW, used for fluorimetric uptake assay, Invitrogen), and biotinylated dextran (10kDa MW, used for immunofluorescent uptake assays, Invitrogen), were diluted in pre-warmed media, added to cells and incubated for time periods and temperatures as described in figure legends. After washing, cells were fixed and subjected to

immunofluorescence analysis as described below. For quantitative analysis of dextran endocytosis, HeLa cells in 35mm dishes were transfected with siRNAs/control siRNAs 48 hours prior to the experiment. Fluorescein isothiocyanate (FITC)-dextran (Sigma-Aldrich) was diluted in media to a concentration of 1mg/ml and added to cells before incubation for 15 minutes at the indicated temperature. Cells were washed twice in media and once in PBS before lysis in 1% NP- 40 in PBS supplemented with protease inhibitors. The lysate was centrifuged at 20,000g for 20 minutes at 4°C and the protein concentration in the supernatant was measured using the BCA Protein Assay Kit (Pierce) for normalization. The amount of FITC-dextran in the supernatant was measured as the emission at 515nm after exciting at 488nm using a FP- 6500 spectrofluorometer with Spectra Manager software (JASCO). The MHC Class I uptake assay was performed according to reference [5]. Briefly, HeLa cells transiently transfected with GFP-tagged GRAF1 or GRAF1 BAR+PH for 16 hours were incubated with W6/32 anti-MHC Class I antibody (American Type Culture Collection) diluted in culture media for 5 or 15 minutes at 37°C to allow endocytosis. Cells were washed in PBS and surface-bound antibody was removed by a 30 second acid wash followed by a wash in culture media to re-adjust the pH. Cells were fixed and MHC Class I was visualised using Alexa568-conjugated antibodies.

**Fixed sample and real time imaging**

For immunofluorescence analysis, HeLa cells were fixed in 3% paraformaldehyde in phosphate-buffered saline (PBS) for 15 minutes at 37°C (to preserve intracellular tubules which are disrupted by fixation at lower temperatures), or 4°C (to demonstrate this temperature dependence), then washed and blocked in 5% goat serum, with 0.1% saponin, in PBS before staining with the appropriate antibodies in 1% goat serum, 0.1% saponin in PBS using standard protocols. Confocal images were taken sequentially using a BioRad Radiance system and LaserSharp software (BioRad). Epifluorescence images were taken using a Zeiss Axioimager Z1 system with AxioVision software. For real time microscopy of the dynamics of GRAF1- and GRAF1 BAR+PH- positive tubules, transfected cells on glass-bottom Petri dishes (WillCo Wells BV, Amsterdam) were washed with buffer (125mM NaCl, 5mM KCl, 10mM D-glucose, 1mM $MgCl_2$, 2mM $CaCl_2$ and 25mM HEPES) and images were taken using a 5-live scanning microscope (Zeiss) or spinning disc confocal system (Improvision) with subsequent analysis in LSM Image Browser (Zeiss), ImageJ (freeware) or Volocity (Improvision). Caveolin1-KO MEFs and control MEFs grown on 12mm coverslips were cotransfected with GFP-GPI and myc-tagged GRAF1 or GRAF1 BAR+PH. Anti-GFP was bound to cells on ice for 30 minutes in unsupplemented $CO_2$-independent medium (Gibco). Cells were washed in $CO_2$-independent medium to remove unbound antibody prior to internalization in pre-warmed growth media (10% foetal bovine serum (Cambrix), 2mM L-glutamine in DMEM (Gibco)) at 37°C, 5% $CO_2$ for 2, 10 or 40 minutes. Post internalization, cells were washed in ice-cold $CO_2$-independent medium and acid stripped using 500mM glycine pH2.2 in ice cold PBS for 1 minute. To remove intensive cytosolic labeling, acid-stripped live cells were permeablized in ice-cold PBS containing 0.05% saponin (Sigma) for 5 minutes. Cells were washed 2 x 1 minute in ice cold PBS before fixation in 2% paraformaldehyde. Internalized anti-GFP was labeled with Alexa Fluor- 660-conjugated goat anti-Rabbit secondary antibody. Myc-tagged GRAF1 FL or BAR+PH was labeled with anti-myc (9B11) primary and Alexa-Fluor-555 goat-anti mouse secondary antibodies. Fluorescence microscopy was carried out using an Axiovert 200m SP LSM 510 META confocal laser-scanning microscope (Zeiss). Images were captured under oil with a 63x plan-APOCHROMAT objective, at appropriate excitation and emission wavelengths. Images were processed using Adobe

Photoshop CS2. Quantification of anti-GFP and GRAF1/GRAF1 BAR+PH colocalization was carried out using Volocity 3.7.0. In brief, target cells were cropped and blue and red channels overlaid to generate a colocalization coefficient based on a percentage of blue voxels that identify with red voxels. Background was subtracted using the automatic threshold feature. Five to seven images across three independent experiments were used to calculate average colocalization and standard error of the mean (SEM). Relative pixel numbers of anti-GFP in each image was calculated in Adobe Photoshop CS2 based on the histogram of each image. For real-time endocytosis experiments, NIH 3T3 cells grown in 35mmM glass bottom dishes were transfected with GFP-tagged GRAF1 or GRAF1 BAR+PH constructs. Cells were washed in ice-cold CO2-independent medium before binding Alexa Fluor-555-conjugated CTxB and/or Alexa Fluor-647-conjugated transferrin for 30 minutes on ice. Appropriate cells were identified using an Axiovert 200m SP LSM 510 META confocal laser-scanning microscope in ice-cold CO2-independent medium. Medium was exchanged for prewarmed CO2-independent medium plus 10% heat-inactivated Serum Supreme and images captured using Lasersharp 2000 4.0. Frames were captured every 10 seconds for 50-100 frames. Images were processed using Image J v1.37 and converted to Quicktime files.

**Supplemental References**


1. Praefcke, G.J., and McMahon, H.T. (2004). The Dynamin superfamily: universal membrane tubulation and fission molecules? Nat. Rev. Mol. Cell Biol. *5*, 133-147.
2. Peter, B.J., Kent, H.M., Mills, I.G., Vallis, Y., Butler, P.J., Evans, P.R., and McMahon, H.T. (2004). BAR domains as sensors of membrane curvature: the amphiphysin BAR structure. Science *303*, 495-499.
3. Motley, A., Bright, N.A., Seaman, M.N., and Robinson, M.S. (2003). Clathrin-mediated endocytosis in AP-2-depleted cells. J. Cell Biol. *162*, 909-918.
4. Kirkham, M., Fujita, A., Chadda, R., Nixon, S.J., Kurzchalia, T.V., Sharma, D.K., Pagano, R.E., Hancock, J.F., Mayor, S., and Parton, R.G. (2005). Ultrastructural identification of uncoated caveolin-independent early endocytic vehicles. J. Cell Biol. *168*, 465-476.
5. Caplan, S., Naslavsky, N., Hartnell, L.M., Lodge, R., Polishchuk, R.S., Donaldson, J.G., and Bonifacino, J.S. (2002). A tubular EHD1-containing compartment involved in the recycling of major histocompatibility complex class I molecules to the plasma membrane. EMBO J. *21*, 2557-2567.

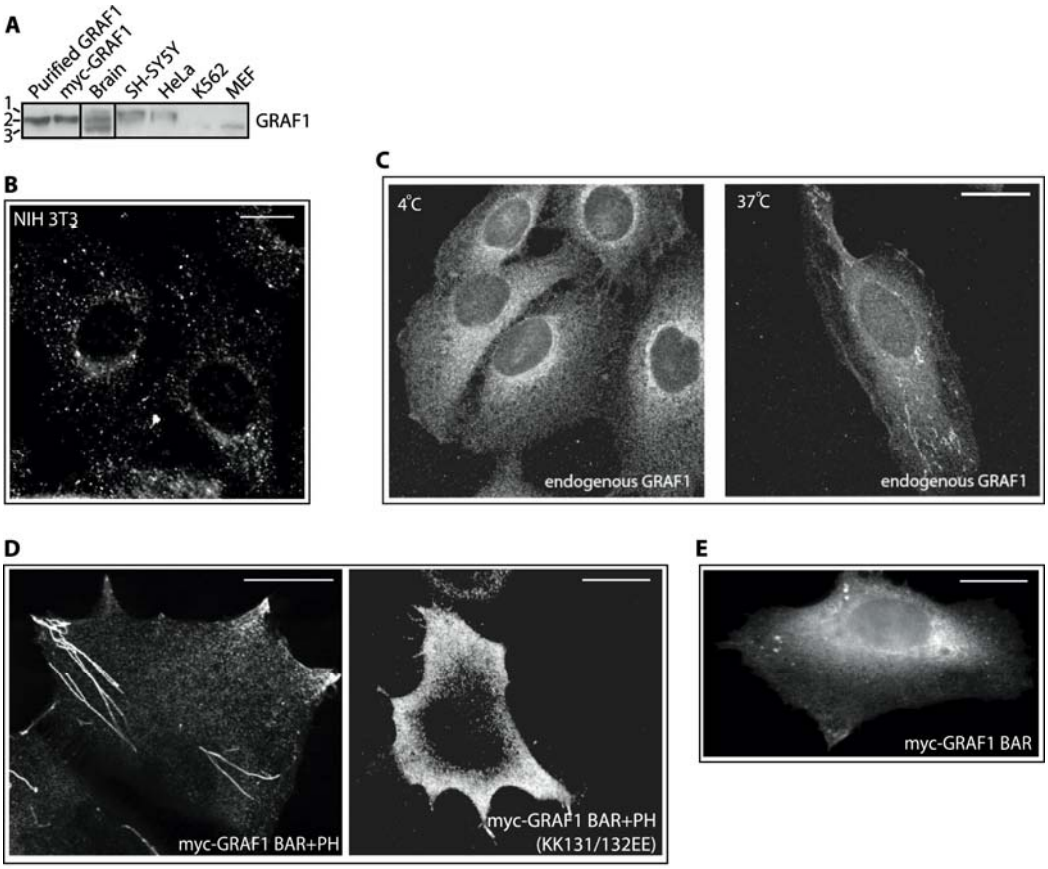


**Figure S1** | **Localisation of GRAF1 to tubular membrane structures is temperature sensitive and dependent on the BAR and PH domains. A,** Western blots showing the different forms of GRAF1 detected in adult rat brain and their differential presence/absence in cultured SH-SY5Y (human neuroblastoma), HeLa (human fibroblast), K562 (human Chronic Myeloid Leukaemia), and MEF (mouse embryonic fibroblast), cells. Western blots of purified GRAF1 and myc-tagged GRAF1 (from lysates of HeLa cells overexpressing this protein) are shown for comparison. **B,** Confocal micrograph of an NIH 3T3 cell stained for endogenous GRAF1 distribution. **C,** Confocal micrographs of HeLa cells fixed either at 4°C or 37°C for 10 minutes in 4% paraformaldehyde and then stained for endogenous GRAF1. Note the absence of GRAF1-positive tubules in the 4°C fixation image. **D**, Confocal micrographs showing the tubular localization of overexpressed myc-tagged GRAF1 BAR+PH protein in HeLa cells and the cytoplasmic localization of a similarly overexpressed protein with a BAR domain mutation (KK131/132EE). **E,** Confocal micrograph showing the cytoplasmic and punctate localization of overexpressed myc-tagged GRAF1 BAR protein in HeLa cells. **Scale bars = 10μm.**

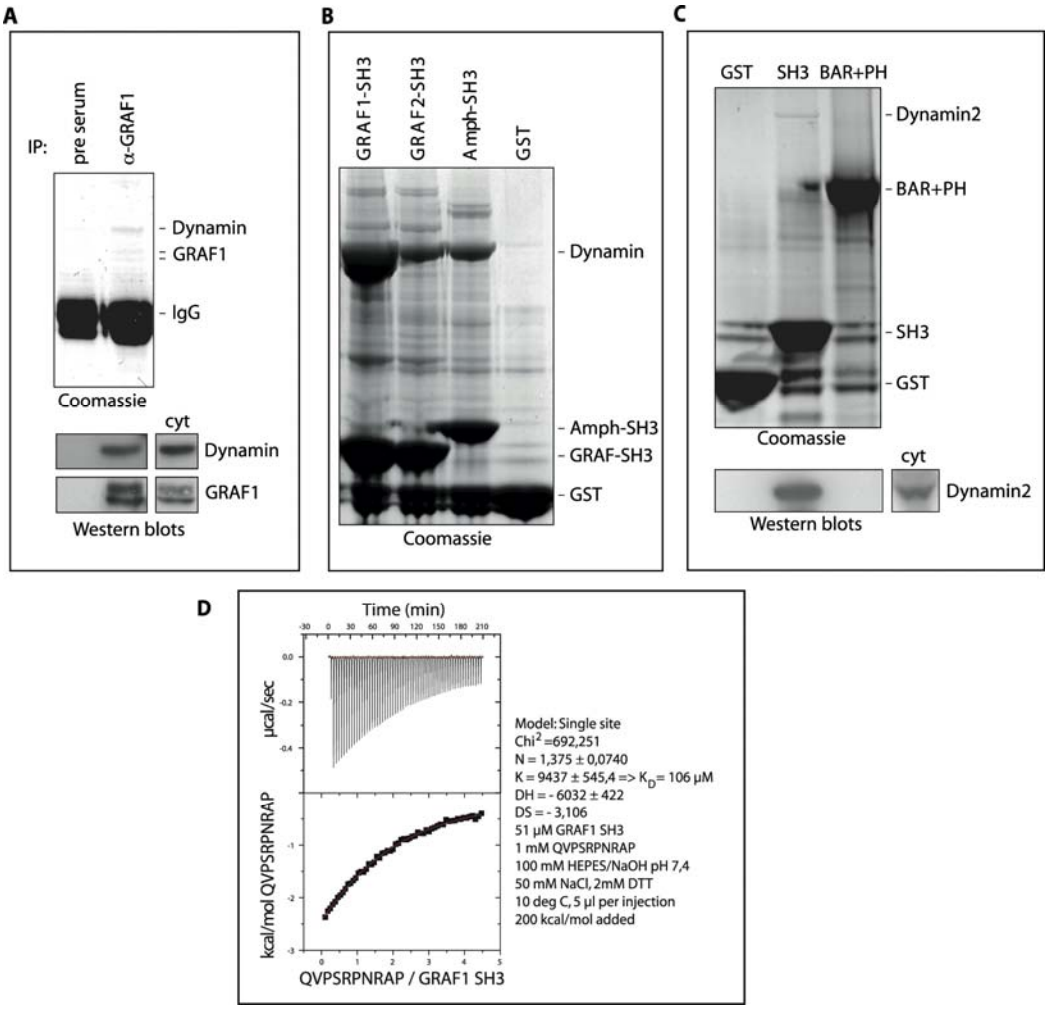


**Figure S2 A-D| Supplementary biochemical data on the binding between GRAF1 and Dynamin. A,** Coomassie-stained gel and confirmatory Western blots of co-immunoprecipitation experiments in rat brain cytosol performed with either control pre-immunization serum (pre-serum) or the Ab3 antibody. Bands in the Coomassie-stained gel were identified by mass spectrometry as described. **B and C,** Coomassie-stained gel and Western blots of pull-down experiments from mouse brain lysate (B) or HeLa cell cytosol (C) with beads bound to GST (control) or GST-tagged GRAF1 BAR+PH, or SH3 proteins. The bands in the Coomassie-stained gel were identified by mass spectrometry as described. Note the major band of Dynamin present in the SH3 lanes, which is not present in the control or BAR+PH condition. 'cyt' marks the HeLa cell lysate (positive control) lane. **D,** The upper panel shows a raw trace from isothermal titration calorimetry performed as described. The lower panel shows the fitting of this data to a one-site binding model from which the affinity (shown) can be calculated. GRAF1 SH3 domain and peptide concentrations, as well as injection volumes and times are shown.

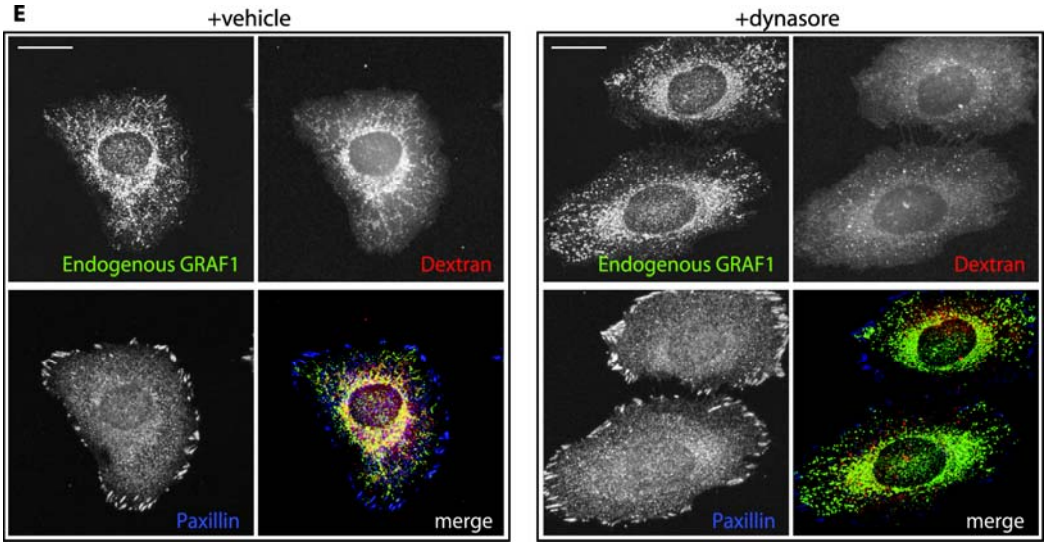


**Figure S2 E** | **Dynasore inhibits the uptake of dextran and affects the localization of GRAF1. E,** Confocal micrographs (maximum projections) of HeLa cells treated with either DMSO (vehicle) or 100μM dynasore for 1 hour before addition of dextran for 15 minutes, fixation, and immunostaining for dextran and the focal adhesion marker paxillin. **Scale bars = 10μm.**

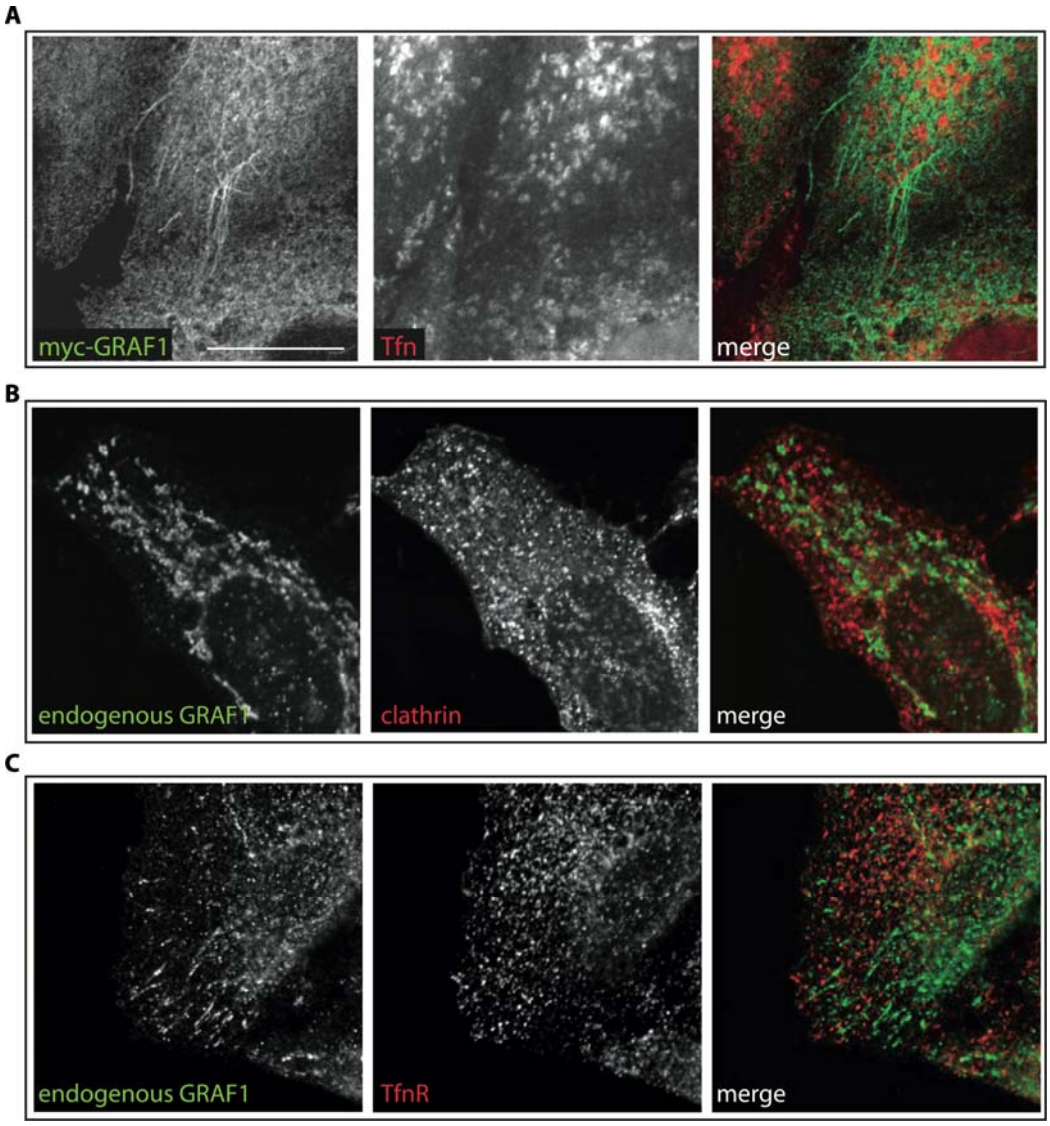


**Figure S3** | **GRAF1-positive endocytic structures are Clathrin-independent and exclude transferrin A-C,** Confocal fluorescent micrographs of HeLa cells stained for endogenous GRAF1 and Clathrin (A), transferrin (B) or transferrin receptor (B). The depicted images are used to show some of the different morphologies of GRAF1-positive structures that are observed in these cells. **Scale bars = 10μm.**

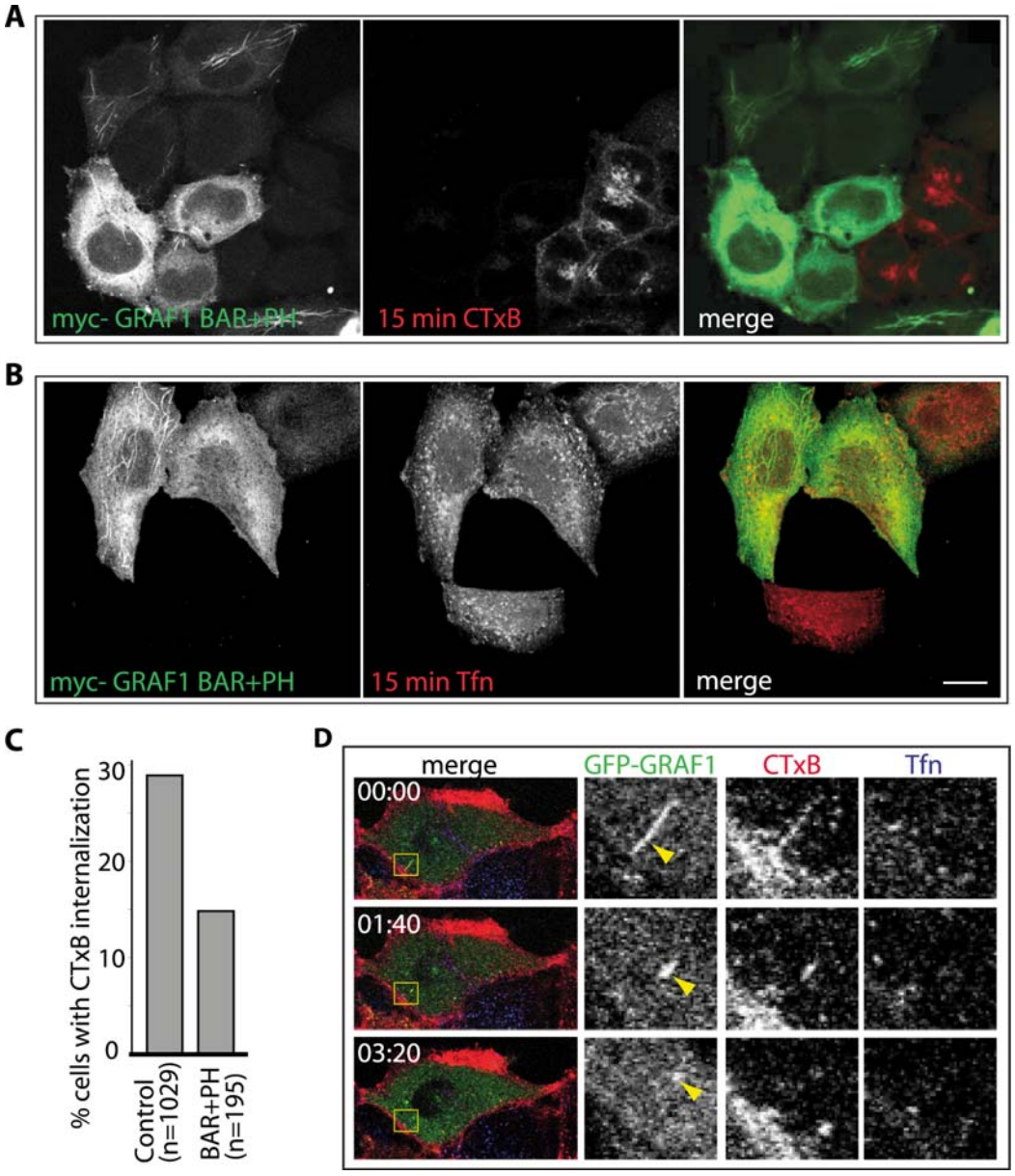


**Figure S4** | **GRAF1 BAR+PH overexpression affects CTxB uptake but not transferrin uptake. A and B,** Confocal micrographs of HeLa cells transfected with myc-tagged GRAF1 BAR+PH and incubated with CTxB or transferrin for 15 minutes before fixation and staining. **C,** The graph shows the quantification of images such as depicted in (A). Cells were scored for expression of GRAF1 BAR+PH (over a threshold corresponding to maximum autofluorescence) and CTxB internalization (over an arbitrarily-set threshold above background). Note the reduction of the number of transfected cells internalising CTxB compared with controls. **D,** Live cell microscopy of NIH 3T3 cells expressing GFP-tagged GRAF1 and incubated with CTxB and transferrin (Tfn) at 4°C before chasing their internalization from the time of warming to 37°C (time=00:00). Note the internalising GRAF1-positive tubule containing CTxB. Note also the lack of colocalization of GRAF1-positive tubules with internalized transferrin. Time is given as minutes:seconds. This sequence is taken from Movie S3. **Scale bars = 10μm.**

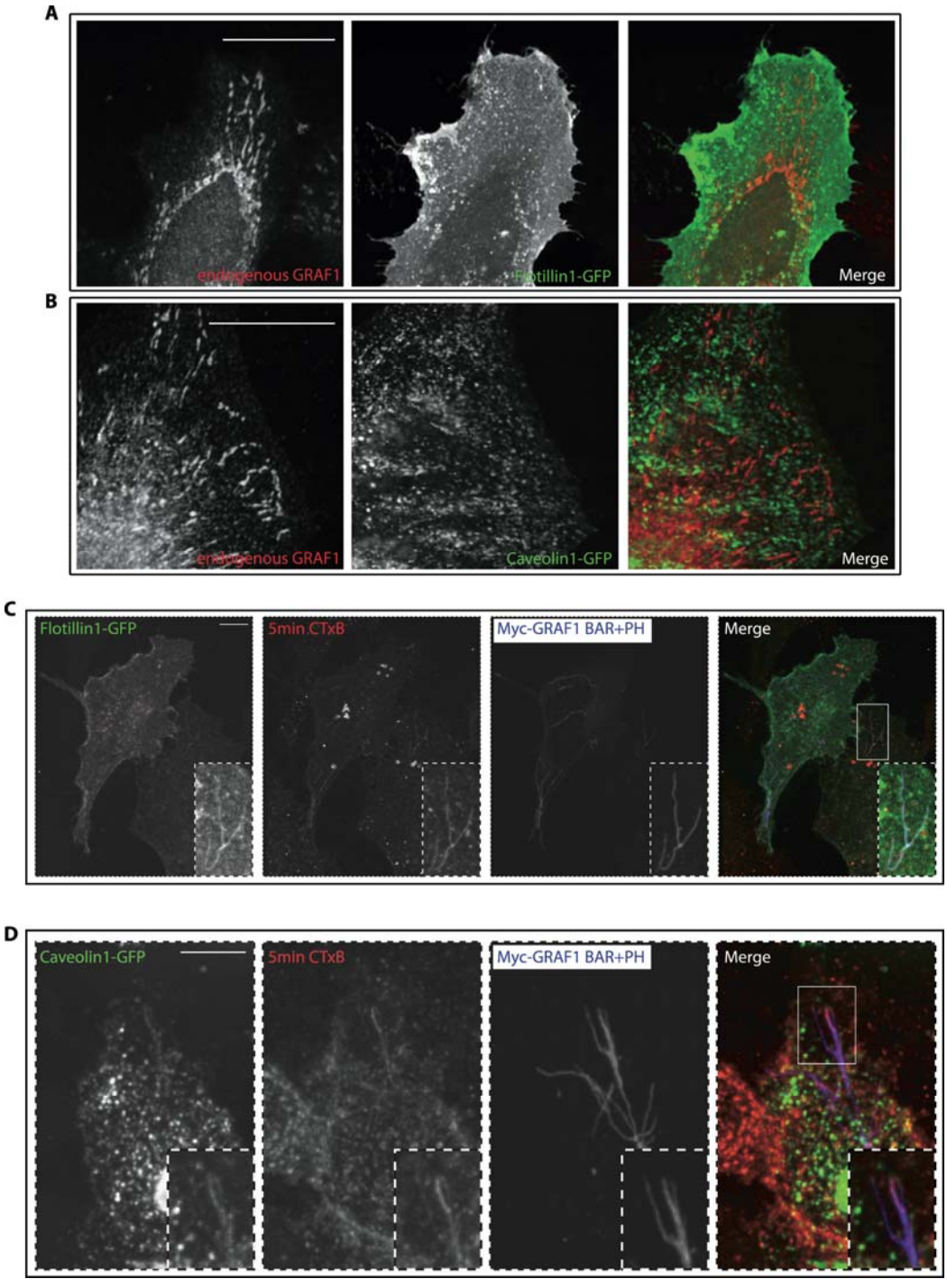


**Figure S5** | **Nature of GRAF1-positive endocytic structures. A and B,** Confocal micrographs of HeLa cells overexpressing GFP-tagged flotillin1 (A) or GFP-tagged caveolin1 (B) and co-stained for endogenous GRAF1. Note the lack of colocalization. **C and D,** Confocal micrographs of HeLa cells overexpressing myc-tagged GRAF1 BAR+PH and flotillin1 (E) or caveolin1 (F) incubated with CTxB for 5 minutes. Note the colocalization of GRAF1 BAR+PH and flotillin1 in CTxB-positive tubular structures. **Scale bars = 10μm.**

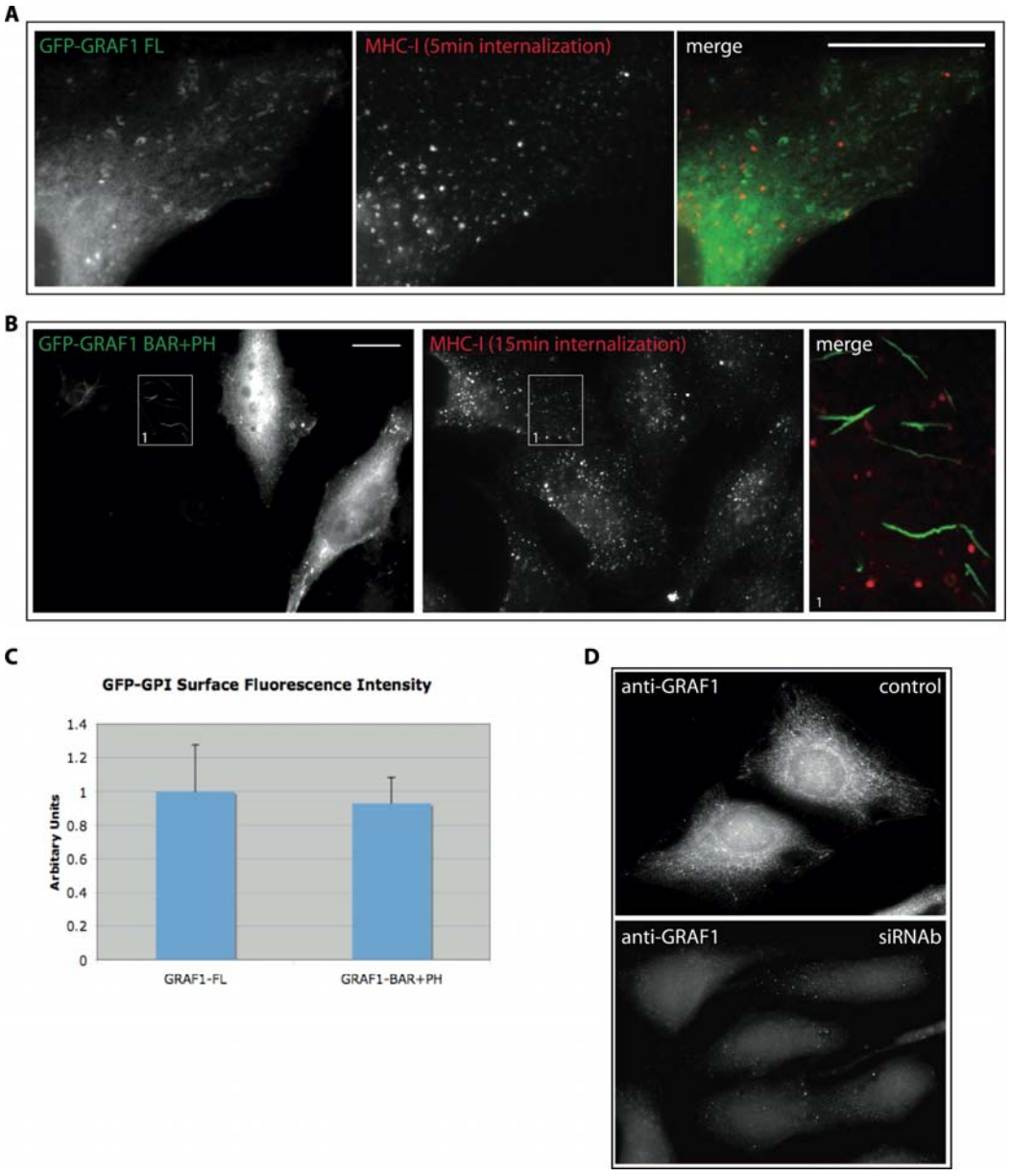


**Figure S6 | GRAF1 BAR+PH overexpression does not affect the uptake of MHC Class I which enter GRAF1-negative compartments. A and B,** Epifluorescence micrographs of HeLa cells, transiently transfected with GFP-tagged GRAF1 FL (A) or GRAF BAR+PH (B) were pulsed with anti-MHC Class I antibody for 5 (A) or 15 minutes (B) at 37°C followed by a brief acid wash to remove surface-bound antibody. MHC Class I was visualized using Alexa568-conjugated secondary antibodies. **C,** Quantitation of surface GFP-GPI levels in cells overexpressing this protein with myc-tagged GRAF1 FL or GRAF1 BAR+PH. **D,** Confocal micrographs of HeLa cells treated with siRNA against GRAF1 or a control siRNA and stained for endocgenous GRAF1. **Scale bars = 10μm.**